

The authors would like to thank the referee for the prompt and precise comments to our reply. We have made modifications and the accompanying reply as follows.

The referee's comments:

Thank you for the rebuttal and providing the additional reference to the publication in the International Journal of Remote Sensing. The idea with the combination of lead data is very good. However, after reading the other paper even more questions arose because the publication also lacks traceability. I would not be able to reproduce your results with the somehow limited information given in the paper. Really important information is missing, some details are even wrong. For example, the used permittivity is not even mentioned. The native SSMI resolution of the 19 GHz channels used in the NASA-Team algorithm (Cavalieri et al. 1996) is about 69x43 not 10 km.

Reply:

With respect to the comment that key information of the L-band radiation model is not available in Zhou et al. (2017), we consider it necessary to formulate a supplementary to describe the model in detail. Specifically, this supplementary includes introduction to the model, including the multi-layer treatment of salinity and temperature profile, sea ice emissivity and permittivity, etc. The modeled L-band brightness temperature (TB) to a range of sea ice parameters for first-year ice (FYI) is also included (Figure S1.a of the supplement), accompanying that for multi-year ice (MYI) in Figure 3c in the manuscript (also Figure S1.b of the supplementary). This supplementary is provided as a supportive document to the original manuscript, and also attached at the end of this reply document.

The following is a concise answer to the referee's question on the permittivity settings in the model: the permittivity of snow, sea ice and sea water mainly follows that in Maaß, et al., (2013). For sea water, an empirical relationship in Klein and Swift (1977) is adopted assuming salinity of 33 g/kg. For sea ice, the permittivity is related to the brine volume fraction, based on Vant et al. (1978) and specific settings in Kaleschke et al. (2010). For snow, same as Maaß, et al. (2013), we adopt fitted parameterization of permittivity as formulated in Tiuri et al., (1984). For the study in this work, under a multi-layer formulation, the salinity structure of MYI (in terms of salinity for each layer) and its effect on permittivity is characterized. The attached supplement provides details of these model settings.

With respect to the comment that a wrong detail of the native SSMI resolution is present in Zhou et al. (2017), we thank the referee and recognize that this is indeed a mistake. We are preparing a corrigendum to the International Journal of Remote Sensing to correct the description, as indicated by the referee: “*Furthermore, sea ice concentration data as used by this article (Cavalieri et al. 1996) are provided on the resolution of 25 km with the native resolution of about 69 km by 43 km*”. For a further reply: other datasets, such as the sea ice concentration based on 89 GHz channel of AMSR-E or AMSR-2 (see Spreen et al., (2008)) serves as candidates for sea ice coverage, which is of about 5 km in nominal resolution. The intention of using sea ice concentration (SIC) in Zhou et al. (2017) is to complement the lead maps in characterizing the effect of (refrozen) open water on the L-band TB of the sea ice cover. Sea ice leads are usually with much small width than the typical passive remote sensing with satellites, and not well represented in the retrieval algorithms for SIC. Therefore, both sea ice lead information and sea ice concentration information are adopted in simulating the TB (see Equation 5 and the last paragraph on page 7075 of Zhou et al., (2017)).

The referee's comments:

Regarding the present manuscript submitted to *The Cryosphere*, I am still not happy with your answers. I still think you could be fooled by circular reasoning. You should split the data into independent "training" and "test" parts to do a real verification, and this for multi-year and first year ice separately. Thereby the very different resolutions and spatial samplings of the sensors involved have to be carefully considered.

The authors would like to make further clarifications on the issue of circular reasoning, and according to the suggestions of the referee, we carry out experiments with different portion of the dataset and show the results.

First, we would like to clarify that the retrieval is based on the snow freeboard (from OIB) and L-band TB (from SMOS), with L-band radiation model and hydrostatic relationship. The L-band model is not trained to the observations of OIB or SMOS. Besides, the model is qualitatively consistent with existing works such as Maaß et al., (2013). The other supportive information for the retrieval is the covariability between snow depth (H_s) and snow freeboard (FB_{snow}), which is based on OIB data on the spatial scale of 40 meters. However, it is important to note that the covariability in the retrieval is only a generic function shape between FB_{snow} and H_s (Equation 3 of the manuscript), and this information does NOT directly specify H_s for any specific FB_{snow} . Instead, under the constraints of both observations (TB and FB_{snow}), the retrieval algorithm seeks the proper value of α that directly decides H_s and Hi . Given typical distribution of FB_{snow} for FYI and MYI (in Figure 1.a below), the scanning of α and the resulting mean snow depth are shown in Figure 1.b. The parameter s that describes the aforementioned covariability (i.e., the function shape parameter) is set to 0.71 and 0.95 for FYI and MYI respectively, which is also adopted in the verification of the original manuscript.

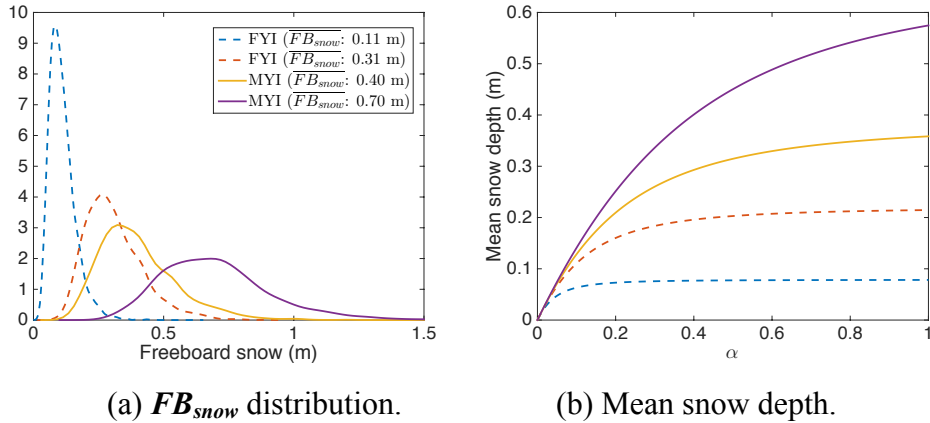
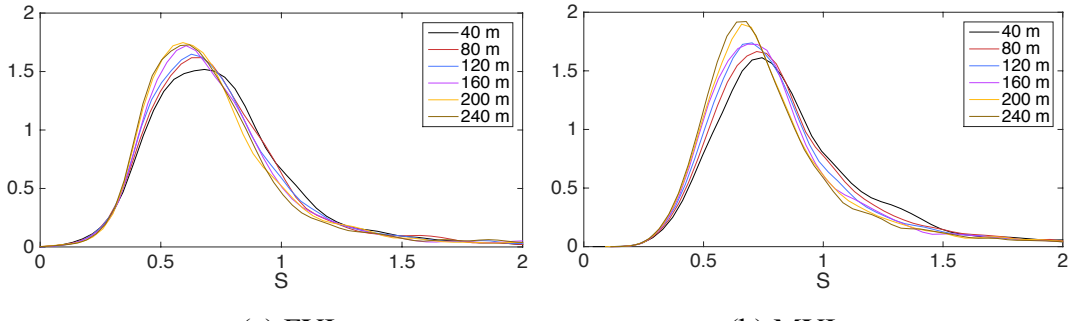


Figure 1. Scanning of parameter α and the corresponding mean snow depth.

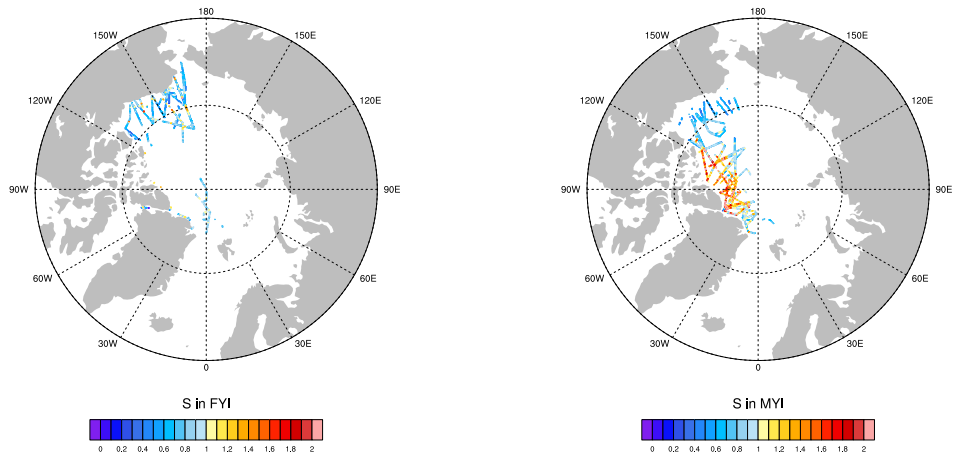
With respect to the difference in the spatial sampling from various sensors as pointed out by the referee, the authors make the following clarifications on how this difference is accounted for during the retrieval, and analyze the relationship to existing satellite laser altimetry. For the retrieval, we assume that the laser altimetry returns the mean value of FB_{snow} on a certain spatial scale. For example, for ICESat, the spatial scale of each laser scan is about 70 meters, which is different from 40 meters of OIB (L4 data). It is worth noting that covariability between H_s and FB_{snow} is present on various spatial scales (Kwok et al., (2011)), and there is indeed scaling of the covariability across different scales (i.e., at different resolution for altimetry). Figure 2 (below)

shows the distribution of s derived from all OIB data on various scales, and there is a slight drift of s to smaller values when manually coarsening the altimetry measurements. This drift applies to both FYI and MYI. Furthermore, in Figure 3 (below), it is shown that there exists distinctive spatial distribution of s for MYI, with the regions north of the Canadian Archipelago featuring $s > 1$. Since for the actual retrieval, the local value of s is not available, in the verification of the original manuscript (Figure 7c and d and corresponding parts), only the global mean value of s is adopted.



(a) FYI. (b) MYI.

Figure 2. Scaling of s derived from OIB data.



(a) FYI.

(b) MYI.

Figure 3. Spatial distribution of s . 40 meter resolution (original OIB) is adopted.

With respect to the suggestions that two separate datasets for “training” and “testing” respectively to ensure independency, the authors have carried out experiments accordingly for further validation of the retrieval. First, the authors would like to clarify that, according to the understanding of the authors, the “training” process mentioned by the referee is the derivation of the value of s . Therefore, we have split all OIB data into years, and use all the data in year 2012 to 2014 to derive s for FYI and for MYI. This process is denoted “training”, and the derived values of s are 0.73 and 1.00 for FYI and MYI, respectively. These values are applied to the retrieval with OIB data in year 2015 (with FB_{snow} from OIB and SMOS TB), which is denoted the process of “testing”. The R^2 of the fitting between the retrieved \mathbf{H}_i (\mathbf{H}_s) to the observed \mathbf{H}_i (\mathbf{H}_s) is 0.88 (0.62) for linear fitting and 0.87 (0.61) for linear fitting line with the constraint that the slope be 1, respectively. The results are also shown in Figure 4 (below), which closely resembles those for the large-scale retrieval in the original manuscript (Figure 7c and d). This provides further verification on the consistency of the nonlinear fitting (in terms of s), and that both \mathbf{H}_i and \mathbf{H}_s can be retrieved

with the proposed method.

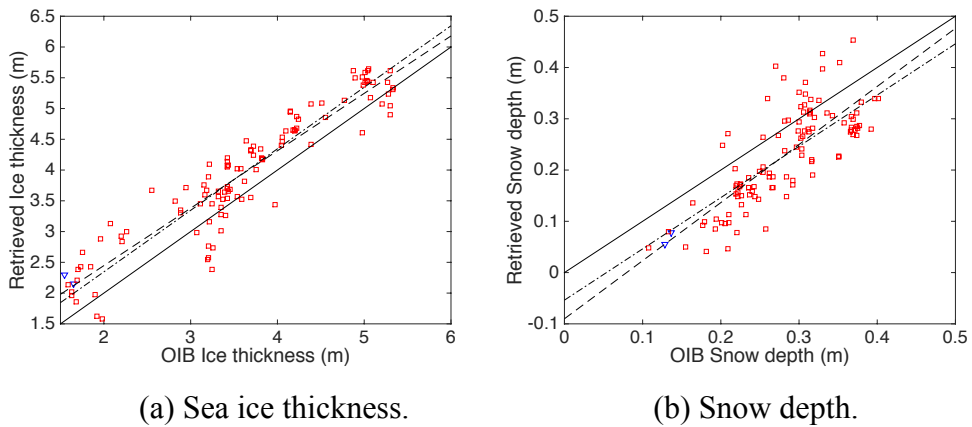


Figure 4. Verification of retrieval in year 2015. OIB data between 2012 and 2014 are used for the derivation of the values of s . The solid line is the 1:1 line and the dashed (dash-dotted) line represents the linear fitting (linear fitting line with the constraint that the slope be 1)

The authors thank the referee, and consider the referee's comments invaluable in making the manuscript clearer and more relevant. We hope that through the responses above, we can fully convey our idea on the retrieval, and would like to answer potential questions from the referee for further clarification. The materials above (including the supplementary material of the radiation model) are considered by the authors to be merged into the original manuscript in its revised form.

References:

- Kaleschke, L., Maaß, N., Haas, C., Hendricks, S., Heygster, G., and Tonboe, R. T.: A sea-ice thickness retrieval model for 1.4 GHz radiometry and application to airborne measurements over low salinity sea-ice, *The Cryosphere*, 4, 583–592, doi:10.5194/tc-4-583-2010, 2010.
- Klein L, Swift C. An improved model for the dielectric constant of sea water at microwave frequencies. *IEEE Journal of Oceanic Engineering*, 1977, 2(1): 104-111.
- Kwok, R., Panzer, B., Leuschen, C., Pang, S., Markus, T., Holt, B., and Gogineni, S.: Airborne surveys of snow depth over Arctic sea ice, *Journal of Geophysical Research: Oceans*, 116, 2011.
- Maaß, N., Kaleschke, L., Tian-Kunze, X., and Drusch, M.: Snow thickness retrieval over thick Arctic sea ice using SMOS satellite data, *The Cryosphere*, 2013, 7, 1971–1989, doi:10.5194/tc-7-1971-2013.
- Spreen, G., L. Kaleschke, and G. Heygster: Sea ice remote sensing using AMSR-E 89 GHz channels. *J. Geophys. Res.*, vol. 113, C02S03, doi:10.1029/2005JC003384.
- Vant, M., Ramseier, R., and Makios, V.: The complex-dielectric constant of sea ice at frequencies in the range 0.1–40 GHz, *J. Appl. Phys.*, 49, 1264–1280, 1978.
- Zhou, L., S. Xu, J. Liu, H. Lu and B. Wang: Improving L-Band Radiation Model and Representation of Small-Scale Variability to Simulate Brightness Temperature of Sea Ice, *International Journal of Remote Sensing*, 2017, 38:23, 7070–7084, doi:10.1080/01431161.2017.1371862.

Supplementary: Description of the L-Band Radiation Model for Sea Ice

The L-band (1.4 GHz) radiation model as used for retrieval describes the radiation emitted from snow covered sea ice that floats over sea water. The model was originally developed for soil moisture applications in Burke et al. (1979), and further adopted for sea ice in Maaß et al. (2013a). As introduced in Zhou et al., (2017), improvements to the model are made to better characterize the vertical structure of the sea ice that is specific to each sea ice type. Details are provided below.

1. General information

The modeling of the radiative properties of the sea ice cover include 4 types of media in the vertical direction: the sea water beneath the sea ice, the sea ice, the snow cover over the sea ice, and the air. The sea water (air) are considered to be semi-infinite beneath (above) the sea ice cover. The sea ice is further divided into N layers in the vertical direction, with each layer of the same height. For the snow cover, a homogeneous structure is assumed, with prescribed thermal conductivity, etc. Besides, dry snow is assumed, and snow morphology features (such as differentiation between wind slab and depth hoar) and similar inhomogeneous vertical structure are not considered. The (SMOS) observed brightness temperature (TB) is assumed to be the multi-angle mean (0-40 degrees) TB as radiated from the aforementioned multi-layer media.

2. Temperature and salinity structure

The radiation model characterizes the vertical structure of the sea ice cover, by specifying the temperature and salinity of each layer, according to other supportive data such as sea ice type, snow surface temperature, etc.

The vertical temperature profile is determined by the overall thermal condition (in terms of the snow surface temperature, T_{surf}), and the thermal conductivity for sea ice (k_{ice}) and that of snow (k_{snow}). The bottom of the sea ice is assumed to be at freezing temperature of -1.8 °C (denoted T_{water}). Based on fittings with observations in Untersteiner (1964) and Yu and Rothrock (1996), the thermal conductivity is defined as:

$$k_{ice} = 2.034 \text{ W m}^{-1} \text{ K}^{-1} + 0.13 \text{ W kg}^{-1} \text{ m}^{-2} \frac{S_{ice}}{T_{ice} - 273.15}$$

$$k_{snow} = 0.31 \text{ W m}^{-1} \text{ K}^{-1}$$

In this study, we consider the change of k_{ice} within the sea ice of minor effects, and use a bulk value for k_{ice} , resulting in a linear temperature profile within the sea ice. This bulk value is determined by the bulk value of S_{ice} . The temperature profile is assumed to be continuous through the media interfaces, and ice temperature is assumed to equal the snow temperature at the snow–ice interface. Given T_{surf} which may be derived from other observations (such as MODIS), the bulk ice and snow temperatures T_{ice} and T_{snow} can be written as:

$$T_{ice} = T_{water} + \frac{1}{2} K(T_{surf} - T_{water}) k_{snow} h_{ice}$$

$$T_{snow} = \frac{1}{2} (T_{water} + T_{surf} + K(T_{surf} - T_{water}) k_{ice} h_{snow})$$

where h_{ice} is the sea ice thickness and h_{snow} is the snow depth and $K = (k_{snow} h_{ice} + k_{ice} h_{snow})^{-1}$. Since a bulk value is adopted for both k_{ice} and k_{snow} , given any T_{surf} , the temperature profile is linear within the snow cover, as well as the sea ice. Then, the temperature of each layer of the sea ice cover can be computed.

For the salinity, sea ice type is considered with differentiation between MYI and FYI. For FYI, the

salinity is assumed to be homogeneous in the vertical direction, and equal the bulk salinity as prescribed by the sea ice thickness. The bulk salinity for FYI is in turn adapted from the multi-linear structure in Cox and Weeks (1974), and defined as follows (where S_{ice} is in ppt):

$$S_{ice} = 6.08 * e^{(-5.81 * h_{ice})} + 7.409 * e^{(-0.5228 * h_{ice})} + 1.5$$

With the deepening of the FYI sea ice cover, the bulk salinity decreases, and its minimum value is kept above 1.5 ppt. On the other hand, for MYI, in order to reflect the effect of brine drainage and flushing during the melt season, a vertical salinity profile is adopted following Schwarzacher et al., (1959). For the k -th sea ice layer, the mean salinity ($S_{i,k}$) is prescribed as:

$$S_{i,k} = \frac{1}{2} S_{max} [1 - \cos(\pi z^{a/(z+b)})]$$

where z is the normalized vertical coordinate with respect to sea ice thickness (starting from 0 on the ice surface to 1 on the ice bottom) and $z = (k - 1/2)/N$, N is number of ice layers, and $S_{max} = 3.2$ ppt, $a=0.407$, $b=0.573$ which are the fitted parameters from in-situ MYI salinity observations. Therefore, for MYI, the sea ice salinity ranges from 0 at the top of the surface ($z = 0$) to S_{max} at the bottom ($z = 1$). The sea water salinity is fixed at constant 33 g/kg.

3. Radiative properties

The radiation model describes the radiation emitted from snow cover, sea ice and sea water, the brightness temperature (TB) at the top of atmospheric (TB_{TOA}) can be described as (Maaß et al., 2013b):

$$TB_{TOA} = (1 - c) * (TB_{water} + (1 - e_{water}) * TB_{cosm}) + c * (TB_{ice} + (1 - e_{ice}) * TB_{cosm}) + \Delta TB_{atm}$$

where c is sea ice concentration, e_{ice} and TB_{ice} the emissivity and TB of sea ice, e_{water} and TB_{water} are the emissivity and TB of sea water, TB_{cosm} is cosmic microwave background radiation, which can be considered as uniform and constant (2.7K). ΔTB_{atm} is TB from atmospheric contribution ranging from -0.36 K and +5.67 K. e_{water} is from the Fresnel equations in different directions of polarization (Ulaby et al., 1981) and e_{ice} is a function of parameters such as polarization, incidence angle, sea ice thickness, temperature, density, salinity, surface roughness, snow depth and temperature, etc.

Based on Maaß et al., (2013a), permittivity of snow (ϵ_{snow}) is determined by a polynomial fit obtained from measurements at microwave frequencies ranging between 840 MHz and 12.6 GHz (Tiuri et al., 1984) as follows:

$$\epsilon_{snow} = (1 + 0.7\rho_{snow} + 0.7\rho_{snow}^2) + i * (1.59 \times 10^6 \times (0.52\rho_{snow} + 0.62\rho_{snow}^2) \times (f^{-1} + 1.23 \times 10^{-14} \sqrt{f}) e^{0.036T})$$

where ρ_{snow} is the relative density of snow (compared to water), T the temperature of snow in degrees Celsius and f the microwave frequency. It should be noted that ϵ_{snow} depend on snow wetness, which is note considered by the model. Permittivity of sea ice (ϵ_{ice}) is confirmed by brine volume fraction (V_b) using empirical relationship in Vant et al., (1978):

$$\epsilon_{ice} = a_1 + a_2 V_b + i * (a_3 + a_4 V_b)$$

where V_b is given in %, and the values of a_1 , a_2 , a_3 , and a_4 following Kaleschke et al., (2010). Similar to Maaß et al. (2013a), for the permittivity of sea water (ϵ_{water}), empirical relationship from Klein and Swift (1977) is adopted and permittivity of air (ϵ_{air}) is assumed to be 1. The brine volume fraction V_b can be expressed in the following (Cox and Weeks, 1983):

$$V_b = \frac{\rho_{ice} S_{ice}}{\rho_{brine} S_{brine} (1 + k)}$$

where S_{ice} is the ice salinity, ρ_{ice} the ice density, S_{brine} the brine salinity and ρ_{brine} the brine density. ρ_{brine} can be fitted with S_{brine} (Cox and Weeks, 1983):

$$\rho_{brine} = 1 + 0.0008 * S_{brine}$$

where S_{brine} is in ‰. Then the following equation is adopted to relate S_{brine} with T_{ice} (Vant et al., 1978):

$$S_{brine} = a + b * T_{ice} + c * T_{ice}^2 + d * T_{ice}^3$$

where T_{ice} is in °C and a, b, c, d are fitted parameters in Vant et al., (1978). These polynomial approximations agreed well with the experimental data of Zubov and Nikolai, (1963).

Also, ρ_{ice} can be expressed by ice temperature (T_{ice} : °C) in Pounder (1965):

$$\rho_{ice} = 0.917 - 1.403 * 10^{-4} T_{ice}$$

Therefore, V_b can be expressed as a function of ρ_{ice} , S_{ice} and T_{ice} .

As derived model from Burke et al. (1979), the radiation model is a non-coherent model. However, the effect of non-coherency is considered to be mitigated by several factors. First, since with the SMOS observations, there exists large variability of both sea ice thickness and snow depth within the typical resolution of 40 km. Second, multi-angle mean of SMOS TB further introduces a range of integration path of radiations. These factors would enable the use of non-coherent model in this study (RMS of Hi variation larger than 1/4 of L-band wavelength, as indicated in Kaleschke et al., (2010)). The multi-layer treatment of the sea ice also explored in Maaß et al. (2013b). With treatment of the salinity profile in MYI (i.e., salinity drainage in the top layers), the modeled TB is more consistent with the SMOS TB, as studied in Zhou et al. (2017).

4. Modeled TB under typical sea ice parameters

Under typical winter Arctic conditions (surface temperature is -30°C), simulated brightness temperature (TB) over different sea ice type from reformulated radiation model shows in Figure S1, along with snow freeboard contour.

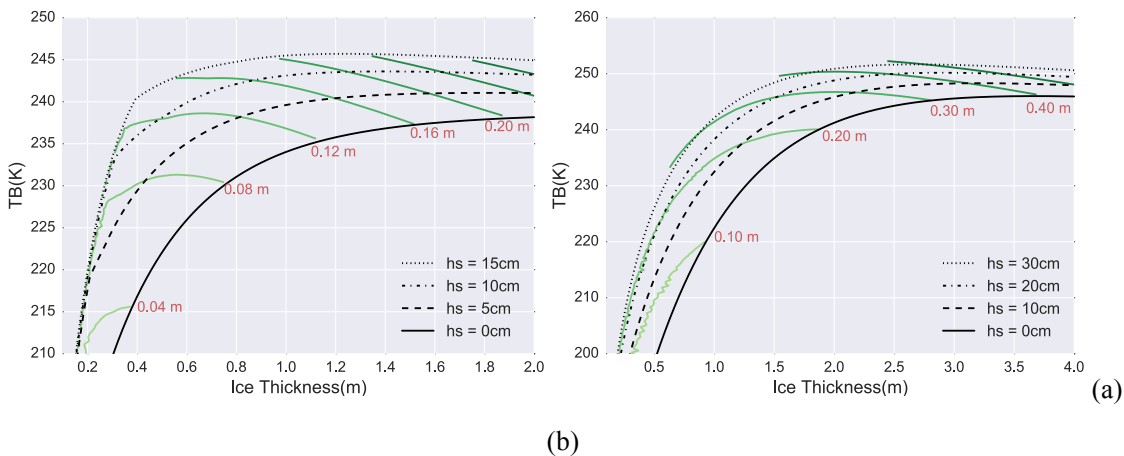


Figure S1. Simulated sea ice surface TB based on reformulated radiation model over FYI (a) and MYI (b). Colored lines are snow freeboard isolines.

References:

- Burke W J, Schmugge T, Paris J F. Comparison of 2.8-and 21-cm microwave radiometer observations over soils with emission model calculations[J]. Journal of Geophysical Research: Oceans, 1979, 84(C1): 287-294.
- Cox G F N, Weeks W F. Salinity variations in sea ice[J]. Journal of Glaciology, 1974, 13(67): 109-120.
- Cox G F N, Weeks W F. Equations for determining the gas and brine volumes in sea-ice samples[J]. Journal of

- Glaciology, 1983, 29(102): 306-316.
- Maaß N, Kaleschke L, Tiankunze X, et al. Snow thickness retrieval over thick Arctic sea ice using SMOS satellite data[J]. *Cryosphere*, 2013a, 7(6):1971-1989.
- Maaß N, Kaleschke L, Stammer D. Remote sensing of sea ice thickness using SMOS data[D]. University of Hamburg Hamburg, 2013b.
- Maykut G A, Untersteiner N. Some results from a time-dependent thermodynamic model of sea ice[J]. *Journal of Geophysical Research*, 1971, 76(6): 1550-1575.
- Kaleschke L, Maaß N, Haas C, et al. A sea-ice thickness retrieval model for 1.4 GHz radiometry and application to airborne measurements over low salinity sea-ice[J]. *The Cryosphere*, 2010, 4(4): 583-592.
- Klein L, Swift C. An improved model for the dielectric constant of sea water at microwave frequencies[J]. *IEEE Journal of Oceanic Engineering*, 1977, 2(1): 104-111.
- Pounder, E.: *The Physics of Ice*, Pergamon Press, the Commonwealth and International Library, Geophysics Division, Oxford, 1965.
- Schwarzacher W. Pack-ice studies in the Arctic Ocean[J]. *Journal of Geophysical Research*, 1959, 64(12): 2357-2367.
- Tiuri M, Sihvola A, Nyfors E, et al. The complex dielectric constant of snow at microwave frequencies[J]. *IEEE Journal of Oceanic Engineering*, 2003, 9(5):377-382.
- Ulaby F T, Moore R K, Fung A K. *Microwave remote sensing: Active and passive. volume 1-microwave remote sensing fundamentals and radiometry*[J]. 1981.
- Untersteiner N. Calculations of temperature regime and heat budget of sea ice in the central Arctic[J]. *Journal of Geophysical Research*, 1964, 69(22): 4755-4766.
- Vant M R, Ramseier R O, Makios V. The complex-dielectric constant of sea ice at frequencies in the range 0.1–40 GHz[J]. *Journal of Applied Physics*, 1978, 49(3):1264-1280.
- Yu Y, Rothrock D A. Thin ice thickness from satellite thermal imagery[J]. *Journal of Geophysical Research: Oceans*, 1996, 101(C11): 25753-25766.
- Zhou L, Xu S, Liu J, et al. Improving L-band radiation model and representation of small-scale variability to simulate brightness temperature of sea ice[J]. *International Journal of Remote Sensing*, 2017, 38(23): 7070-7084.
- Zubov, Nikolai Nikolaevich. *Arctic ice*. Naval Oceanographic Office Washington DC, 1963.